Effect of the loam inter-layer on the migration and breakthrough of benzene under constant flow in the unsaturated zone: column experiments

Leilei Guo, Lin Qian, Mo Xu, Yunhui Zhang, Xiaobing Kang, Xianxuan Xiao and Qiang Zhang

ABSTRACT

The reliable prediction of transport and attenuation of dissolved-phase contamination in the unsaturated zone is a complex and multi-process problem. Based on the adsorption properties of soil samples to solutes, the soil column test and laboratory analysis were carried out in this study. The effects of the loam inter-layer on the migration and breakthrough of the characteristic pollutant benzene and non-absorbent Br^- were studied. The results showed that the relatively high clay content of the inter-layer significantly changed the BTC (breakthrough curve). It not only delayed the migration time of benzene into the aquifer but also to some extent produced an attenuation effect, effectively reducing the content of the characteristic pollutants through the unsaturated zone. The dispersion coefficient was obtained through the measured Br^-. The theoretical values were calculated and compared with the experimental data by using a one-dimensional unsaturated solute transport equation. The result was basically consistent, which proved the validity and reliability of the model. Through the BTC of benzene, the retardation factor was obtained and used to describe the influence of the loam inter-layer on the migration and breakthrough, which could provide the basis for the accurate modeling of groundwater remediation projects.

Key words | adsorption, benzene, breakthrough curve, retardation factor, soil, unsaturated zone

Leilei Guo
Lin Qian
Mo Xu (corresponding author)
Yunhui Zhang
Xiaobing Kang
Xianxuan Xiao
Qiang Zhang
State Key Laboratory of Geohazard Prevention and Geoenvironment Protection,
Chengdu University of Technology,
Chengdu, 610059,
China
E-mail: xm@cdut.edu.cn

INTRODUCTION

Groundwater organic contamination has recently become a research hotspot in the groundwater field. Once groundwater is polluted, it is very difficult to manage and requires extensive time and funds (Flathman *et al.* 1994; Aral 1995). The pollution of aquifers is a slow process with accumulation and lagging. Additionally, as is the case for groundwater pollution caused by contaminated fluid percolating from landfill sites, it may not even be detected for decades (Appelo 1994). The transformation and form of its migration and occurrence are influenced by its own nature and the surrounding geological environment; for example, the water sources, the soil texture, the soil structure, the solubility of the pollutant, and geochemical variables such as salt content (Walter *et al.* 2000; Yang & Yanful 2002; Kampe *et al.* 2003; Ayotamuno *et al.* 2006; Ma *et al.* 2018).

The unsaturated zone has been considered a necessary channel for contaminants to enter the groundwater; hence, information on the migration and breakthrough of organic pollution through it is crucial. To fully capture the pollutants within a layered porous medium, a 'permeable reactive barrier' has often been used. The contaminants' remediation was then assessed using physical, chemical and biochemical means to intercept, fix or degrade them (Porro *et al.* 1993; Blowes *et al.* 1997; Suthersan 2002; Mahmoodlu *et al.* 2014). Zhang *et al.* (2017) constructed a barrier over a waste site for two decades and demonstrated its effectiveness. The barrier was tested, and the surface-barrier performance was rigorously evaluated. We can derive insights from this method to simulate the migration and breakthrough of VOCs (volatile organic compounds) through the barrier.

As common organic pollutants, VOCs, which are toxic, volatile and non-hydrophilic, and their unsaturated-zone transport and attenuation, have attracted increased attention (Ronen *et al.* 2005; Fetter 2011). Rivett *et al.* (2011) and

Abbas et al. (2012) predicted the status of VOCs in unsaturated soils by developing a model using controlled laboratory tests, field datasets and model sensitivity analysis. Therefore, laboratory testing is one of the keys to conducting an integrated assessment. In the laboratory, soil columns have been used to carry out organic matter migration experiments. For instance, Song et al. (2018) studied oestrogens based upon gas chromatography, with a focus on their penetration from the soil surface to the groundwater and detected that the concentrations changed abruptly at the interface of layers. Moreover, Khan et al. (2016) analysed the VOC biodegradation rate by using Fick's law in a laboratory setup that mimicked the unsaturated zone. The abovementioned literature provided good guidance for how to carry out our test.

However, few studies have focused upon the migration and breakthrough of benzene, especially in sandy soil containing a loam inter-layer. To consider how it could obstruct the contaminants, we designed the loam inter-layer as the 'barrier'. We carried out the Br^- tracer test and benzene breakthrough test under a constant flow rate in two kinds of soil columns, after which we created the breakthrough curves and fitted the convection-dispersion model. To analyse the migration, we set the concentration of Br^- at 5 mg/L, and benzene, as the characteristic pollutant, at 5 mg/L. The adsorption behaviour of benzene and Br^- in the samples were observed, and the adsorption equilibrium time and the maximum adsorption capacity were determined by gas chromatography. Based on the above

basic experiments, we investigated the actual column flow rate, the variation in matrix potential, the distribution coefficients, and the retardation factor to discuss the effect of the loam inter-layer on benzene and Br^- migration as well as their penetration of the unsaturated zone.

MATERIALS AND METHODS

Experimental facility and materials

A Plexiglas column was used as the reactor (60 cm high, 15 cm ID), and the results were obtained through an online system with moisture transducers and matrix potential sensors connected through the data collector, which monitored the water content and the soil water potential respectively (Figure 1). We set the 1# soil column as the homogeneous fine sand column, and the 2# soil column with a silty loam inter-layer at a depth of 40–45 cm. The sample holes were made on the sides of the columns. The syringe needles were evenly distributed at the top of the device to simulate natural rainfall. The water inlet was connected to a peristaltic pump to ensure the sufficient provision of water. The sealant was applied at the junction of the device to simulate the non-evaporation condition for benzene. The bottom 5 cm of the device was filled with a dry silica sand and gravel layer to prevent the blocking of the lower tube by the accumulation of the leachate.
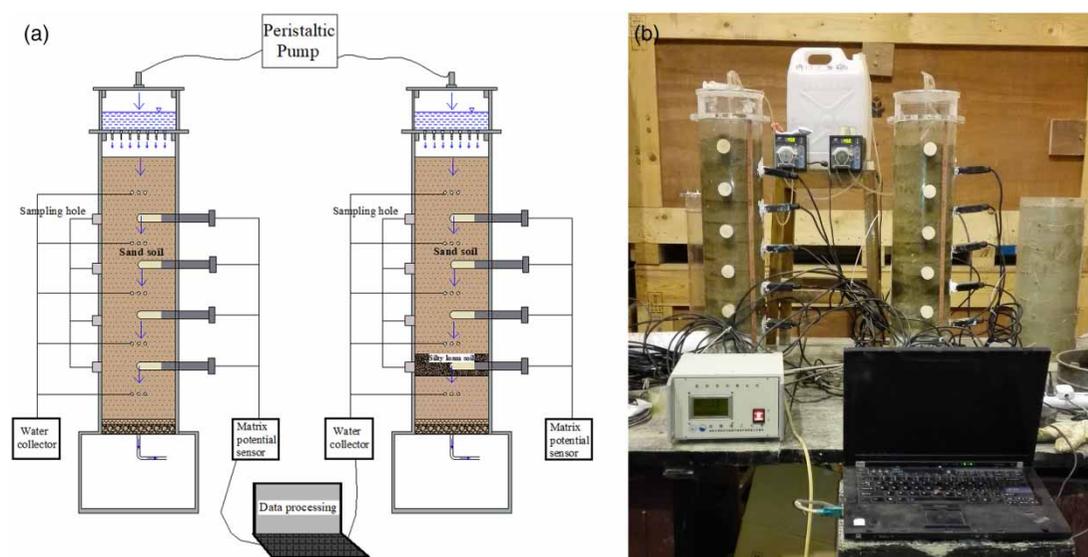

Figure 1 | (a) Schematic of the experiment device; (b) photograph of the soil column and the main data acquisition equipment.

The silt loam soil was taken from a construction foundation pit in Jinniu District, Chengdu, and the sand was river sand. The original soil was spread out in the room, dried and crushed. The impurities, such as grass roots and stone, were removed and passed through a 2 mm screen. The soil was then placed in an oven at 105 °C for 24 h. The Mastersizer 2000 was used to analyse the soil sample particles, which were categorized according to the international soil division standard. The analysis of soil particle size and the results on the physical parameters are shown in Table 1.

The main chemicals were benzene (analysis pure), NaBr (chromatographically pure), and deionized water. The main instruments are shown in Table 2.

Experimental design

Isotherm test

Due to the high clay content of silty loam and the negative charge on the surface of soil, the adsorption behaviour of Br^- in sand soil and silty loam soil was quantitatively analysed through a static isothermal adsorption test. The Br^- absorbability test was conducted as follows. Soil sample:

Table 1 | Soil particle composition and physical parameters

Sample	Sand % (>0.02 mm)	Silt% (0.002– 0.02 mm)	Clay % (0–0.002 mm)	K_s (m/d)
Sand soil	87.36	9.88	2.76	11.5
Silty loam soil	26.75	62.29	5.96	7.957×10^{-3}

Ks: the permeability coefficient of the soil.

Table 2 | Main instrument of benzene adsorption experiment

Instrument	Specifications	Function
GC7890 meteorological chromatography	LLD: 0.05 mg/L	Benzene measurement
CHZ82 thermostat oscillator	$0 \sim 300$RPM; room temperature $\sim$ 50 °C	Constant temperature oscillation for adsorption experiments
Laboratory ultra-pure water apparatus	/	Provide deionized water
861 Advanced compact IC	LLD: 2 µg/L	Br^- measurement

LLD: low limit of detection; RPM: revolutions per minute.

20 g; reactor: conical flask of 250 ml; solution: 100 ml; the initial concentrations of Br^- were set as 1 g/L, 2 g/L, 5 g/L, 10 g/L and 20 g/L; the flask was sealed, covered and oscillated at a constant temperature at 200 rpm for 2 h in the CHZ82 thermostat oscillator; the water samples were filtrated through a polyvinylidene fluoride membrane (Millipore 0.45 µm); then the Br^- was measured by the 861 Advanced compact IC.

As benzene is a non-conservative substance, we carried out isothermal kinetic adsorption experiments. Benzene solution: 6 mg/L, 50 ml; soil sample: 2 g; reactor: 100 mL headspace bottle; sealed, covered and oscillated with constant temperature at 200 rpm; measured by GC7890 meteorological chromatography at 0.5, 2, 5, 10, 24, and 48 h, respectively. We determined the adsorption model, adsorption equilibrium time and maximum adsorption capacity.

Henry, Langmuir, and Freundlich models were fitted to the equilibrium data. 2 g of the sandy and silty loam were placed in six 100 ml head-space bottles, and then 50 ml of benzene solution at 4 mg/L, 8 mg/L, 12 mg/L, 16 mg/L and 20 mg/L initial concentrations were added; oscillated and measured after 48 h.

It was also necessary to verify whether the inorganic components in the groundwater had affected the adsorption of benzene in the soil. The effects of different concentrations of Br^- on benzene adsorption were analysed. Benzene initial concentrations were 2, 4, 6, 8, and 10 mg/L. reactor: 100 mL head-space bottle; soil sample: 2 g; sealed and oscillated at 10 °C; oscillated and measured after 48 h.

Column test

To fill the soil columns with a bulk density similar to the natural medium, the fine sand used was 1.5 g/cm³ and the silty loam was 1.3 g/cm³. To avoid artificial stratification, the surface of each layer of soil was made rough, and the soil column was filled with layers of 5 cm each. The 1# soil column was set as the homogeneous fine sand. The 2# soil column was added as a silty loam inter-layer at the depth of 40–45 cm (Figure 1). The quartz sand at the bottom of the column, with a thickness of 1 cm, ensured uniform precipitation. Constant flow rainfall was simulated for the concentration of Br^- and benzene at 5 mg/L through the peristaltic pump. The concentrations of water content, benzene and Br^- in the soil samples were detected. When the solution penetrated the soil column, the breakthrough time was recorded, and the leachate was detected. Then, the breakthrough curves of Br^- and benzene were drawn and analysed. The experiment was stopped when the concentration of benzene stabilized.

VGM model and characteristic parameters

To fit the water characteristic curve and calculate the unsaturated water conductivity, we chose the Van Genuchten equation (Van Genuchten 1980).

$$\theta_h = \theta_r + \frac{\theta_s - \theta_r}{[1 + (\alpha \cdot h)^n]^m} \tag{1}$$

where θ_h is the volumetric soil water content, cm^3/cm^3; h is pressure head, -cm; θ_s is the saturated volume moisture content; θ_r is the residual volume moisture content; α and n are empirical fitting parameters; and m = 1–1/n.

The pressure membrane plate method was used to obtain the parameters of the water characteristics. The method was used to measure matrix potential by a porous ceramic plate in which the pore could only pass through the water but not the air. The instrument consists of an adjustable air pressure input device and a pressure chamber, in which a pressure plate (porous ceramic plate) was installed. First, we saturated soil samples by using a cutting ring. The saturated soil samples were placed in the chamber and pressurized, which caused the water to flow out of the soil, and the water content was measured (moisture content). A series of corresponding moisture content data could be obtained from different pressures. The soil water suction was used to replace the pressure head. The volume of water content was replaced by gravity water content. The lsqcurvefit function and curvilinear regression (nlilfit and nlintool) in MATLAB were used to solve the equation. The calculated parameters are shown in Table 3.

Adsorption isotherms

Equilibrium isotherms are very important for understanding adsorption systems. The quantity of adsorption was calculated as follows (Franco *et al.* 2017):

$$q = V(C_0 - C_e)/m \tag{2}$$

where q is the amount of solute adsorbed on the soil, mg/g; V is the volume of the solution, ml; C_0 and C_e are the liquid-phase concentrations at the initial and equilibrium conditions respectively, mg/L; and m is the mass of soil, g.

The isotherm equations of Henry (Equations (3) and (4)) were widely used to fit the adsorption curve of Br^- (Parker & Van Genuchten 1984).

$$C_s = K C_e^n \tag{3}$$

take the logarithm of both sides:

$$lgC_s = lgK + nlgC_e \tag{4}$$

where C_s is the attachment concentration in the absorbent, $\mu g/g$; K is the adsorption constant; n is a nonlinear degree parameter. A value of $1/n > 1$ suggests a weak adsorption bond between the molecules on the adsorbents; on the other hand, a value of $1/n < 1$ suggests a strong adsorption bond as a result of strong intermolecular attraction within the adsorbent layers (Duong 1992; Nanta *et al.* 2018).

The isotherm equations of Henry (Equation (5)), Langmuir (Equation (6)) and Freundlich (Equation (7)) were used to fit the adsorption curve of benzene (Sander 2015; Franco *et al.* 2017).

$$Q_e = K_H \cdot C_e \tag{5}$$

$$\frac{C_e}{Q_e} = \frac{C_e}{Q_{max}} + \frac{1}{K_L \cdot Q_{max}} \tag{6}$$

$$Q_e = K_F C_e^{1/n} \tag{7}$$

Q_{max} is the maximum amount of benzene adsorbed, mg/kg; and Q_e is the adsorbed amount at equilibrium, mg/g. K_L is the Henry constant ; K_L is the constant related to the free energy of the adsorption, L/mg; K_F ($(mg/g)(L/mg)^{1/n}$) and n are Freundlich constants that give a measure of adsorption capacity and adsorption intensity.

Breakthrough curves model and dispersion coefficient

The combined advection-diffusion equation (CDE) can describe the migration characteristics of the solute. The one-dimensional unsaturated solute transport equation without considering other sources (Gianfilippo *et al.* 2016):

$$\frac{\partial C}{\partial t} = D\frac{\partial^2 C}{\partial x^2} - v\frac{\partial C}{\partial x} \tag{8}$$

initial conditions:

$$\begin{cases} C(x, 0) = C_i(x > 0) \\ C(0, t) = C_0(t > 0) \\ C(\infty, 0) = 0(t > 0) \end{cases} \tag{9}$$

Table 3 | Fitted values of soil moisture characteristic curve

Fitted data	θ_r	θ_s	α	n	Resnorm
Silty loam soil	0.0319	0.3705	0.0410	1.8103	2.5649e-004
Sand soil	0.0177	0.2603	0.2386	1.3572	1.2898e-004

boundary conditions:

$$\left[-D\frac{\partial C}{\partial x} + vC \right] = vC_0 \qquad (10)$$

where v is the average pore water velocity, cm/h; C_i is the background concentration of the solute in the soil, mg/L; D is the hydrodynamic dispersion coefficient, cm^2/h; C_0 is the initial injection concentration, mg/L; C is the soil retention concentration, mg/L; x is the distance, cm; and t is the time, h.

For one-dimensional unsaturated solute migration, the analytical solution of the CDE is:

$$C(x, \ t) = \frac{C_0}{2} \left\{ \text{erfc} \left(r\frac{x - vt}{2\sqrt{Dt}} \right) + \exp\left(\frac{vx}{D}\right) \text{erfc}\left(\frac{x + vt}{2\sqrt{Dt}}\right) \right\} \qquad (11)$$

Because the value of the second term within curly brackets is very small, it can be ignored; erfc is a residual error function:

$$C(x, \ t) = \frac{C_0}{2} \text{erfc}\left(\frac{x-vt}{2\sqrt{Dt}}\right) \qquad (12)$$

after deformation:

$$\frac{C(x, \ t)}{C_0} = 1 - N\left(\frac{x-vt}{2\sqrt{Dt}}\right) \qquad (13)$$

where $N\left(\frac{x - vt}{\sqrt{2Dt}}\right)$ is the normal distribution with mean vt and $\sqrt{2Dt}$ is the standard deviation.

Using the characteristics of the normal distribution function, we located the corresponding times $t_{0.16}$ ($C/C_0 = 0.16$) and $t_{0.84}$ ($C/C_0 = 0.84$) on the breakthrough curve. Then we used the fact that one standard deviation (equal to $\sqrt{2Dt}$) encompasses 68% of the probability and derived the dispersion coefficient D from there.

$$D = \frac{1}{8}\left[\frac{1 - vt_{0.16}}{\sqrt{t_{0.16}}} - \frac{1 - vt_{0.84}}{\sqrt{t_{0.84}}} \right]^2 \qquad (14)$$

Retardation factor

The adsorption and desorption of VOCs in soil were the most important mechanisms for contaminant transport. Under the condition of mass exchange balance, the retardation factor can be used to describe the effect of interphase exchange and partitioning on solute transport. In the solute transport of groundwater, the retardation factor can be explained as the ratio of the seepage velocity to the observed velocity of the adsorbent. Br$^-$ as a conservative ion has low absorbability, and the retardation factor R = 1 (Parker & Van Genuchten 1984). In the seepage column experiment, it can be explained as the ratio of the breakthrough time of the adsorptive tracer to the non-adsorptive tracer. According to the experimental results, the retardation factor was approximately calculated as follows.

$$R = t_c^* / t_c \qquad (15)$$

where R is the retardation factor; t_c^* is the absorbent tracer piston flow arrival time; t_c is the non-adsorbable tracer arrival time.

RESULTS AND DISCUSSION

Absorbability analysis of Br$^-$

To represent the extent of Br$^-$ absorbability in the sandy and silty clay soil, Equation (4) was used. The lgCe – lgCs curves and the determination coefficients (R^2) are shown in Table 4.

According to Table 4, the data showed that the adsorption of Br$^-$ to the soils was negligible. As a conservative ion, it was thus reasonable to choose Br$^-$ as the flow tracer for this experiment.

Absorbability analysis of benzene

The adsorption equilibrium studies were performed to evaluate the performance of soils for benzene adsorption. The isotherm of adsorption is shown in Figure 2.

The adsorption capacity can be greatly influenced by soil texture, such as clay content (Krishna *et al.* 2001; Cooper *et al.* 2010). The average adsorption capacity of VOCs by modified soil has been discussed (Lo *et al.* 1997; Gullick & Weber 2001; Bartelt-Hunt *et al.* 2005). The

Table 4 | lgCe-lgCs fitting curve of Br$^-$

Sample	Fitting: *lgCs-lgCe*	1/n	R^2
Sand soil	$lgCs = 0.0469 lgCe + 0.1149$	21.32	0.9899
Silty loam soil	$lgCs = 0.1035 lgCe + 0.1753$	9.66	0.9963
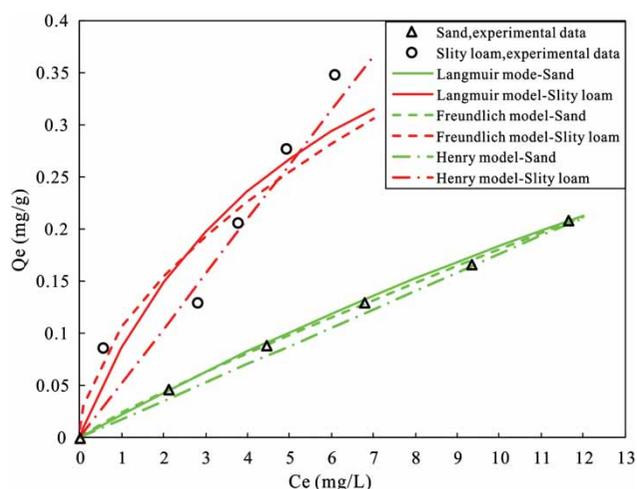
Figure 2 │ Langmuir, Freundlich and Henry adsorption isotherms of benzene.

increases the pore and adsorption sites, which play an important role in the adsorption, increasing the adsorption capacity and medium distribution coefficient.

The isotherm model was essential to elucidate the adsorption behaviour and to obtain information regarding the adsorption mechanism. Thus, three isotherm models (Equations (5)–(7)) were fitted to the equilibrium data (Figure 2). The estimation of the parameters and the determination coefficients (R^2) are summarized in Table 5.

According to Table 5, the experimental data were best fitted by the Henry isotherm. Ronen *et al.* (2005) determined that the relationship between the gas and liquid equilibria followed Henry's Law. The adsorption model of clay on benzene showed a highly linear relationship (Sheng *et al.* 1996). Based on linear adsorption, the degree of fit of the Henry model was the highest, and the adsorption capacity of silty loam was higher than that of sand. With the increased particle density, the distribution coefficient of the soil decreased significantly (Wambold 1993). The higher the contents of clay and organic matter are, the weaker the migration of the pollutants.

The effects of different concentrations of Br^- on benzene adsorption are shown in Figure 3.

The adsorption capacity of benzene showed a slight downward trend with increased Br^-, especially when it was greater than 6 mg/L. This is mostly due to the

adsorption process of VOCs in the water-bearing system is as follows. VOCs, as the non-conserved component, dissolved into the water phase and were then adsorbed (Petersen *et al.* 1994; Unger *et al.* 1996). Due to the non-polarity of the VOCs, the essence of the adsorption was the distribution process of the pollution constituent and its molecular structure. Soil surface organic matter usually has complex surface functional groups, which greatly

Table 5 │ Parameters of the isotherm adsorption of the Henry, Langmuir, and Freundlich models

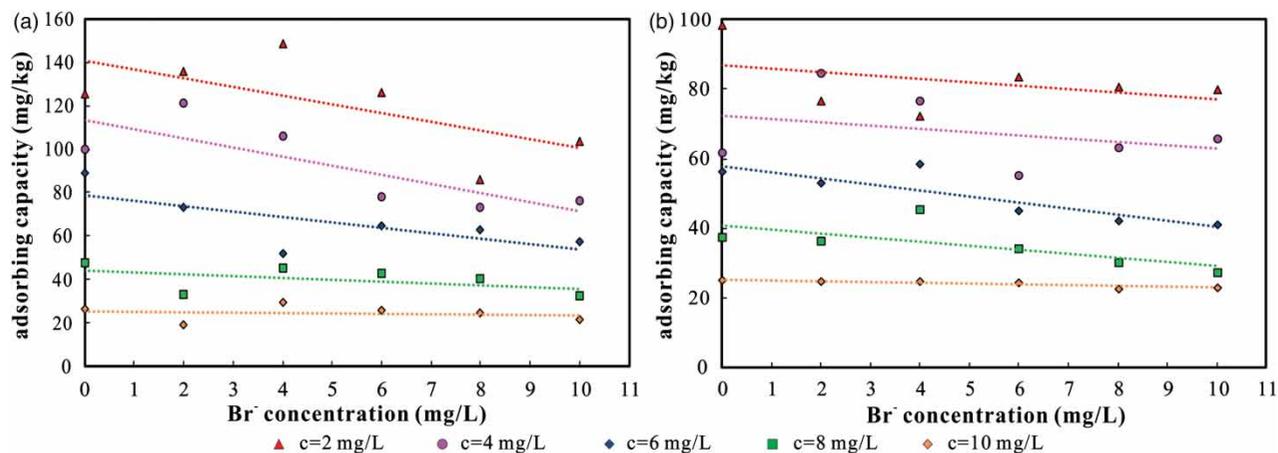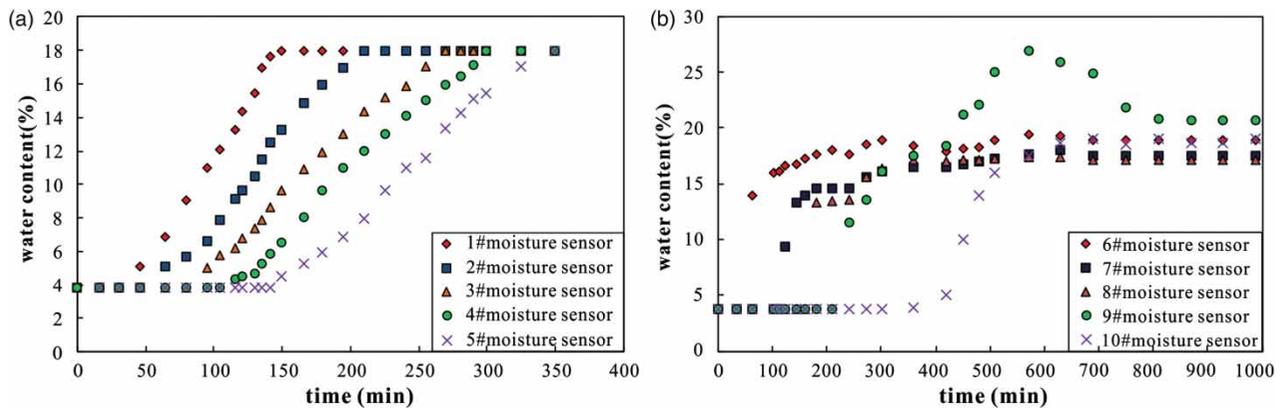| Medium type	Henry		Langmuir			Freundlich		
	K_H	R^2	K_L	Q_{max}	R^2	K_F	n	R^2
Sandy soil	0.0176	0.9965	0.025	0.909	0.9058	0.024	1.145	0.9994
Silty loam soil	0.0523	0.9594	0.178	0.568	0.412	0.107	1.847	0.8457

Figure 3 │ Benzene adsorption capacity on the sand soil (a) and silty loam soil (b) under different Br^- concentrations.

Figure 4 | Water content distribution characteristics of the 1# soil column (a) and 2# soil column (b).

micropores in solids that only allow small organic molecules to enter. When the concentration of benzene was low, the medium surface pore adsorption point was enough to satisfy the requirements for adsorption. However, when Br^- was high, the adsorption point would have been affected, and as a result, the capacity for benzene adsorption would gradually decrease. In summary, this effect was generally small, indicating that the effect of the Br^- on benzene adsorption and migration is relatively small.

Migration law

Since water was the transport carrier of the solute, the moisture content of the unsaturated zone directly affects the solute transport. The characteristics of the variation in moisture content are shown in Figure 4. We determined the soil moisture content by the soil dielectric permittivity (Onsy *et al.* 2017).

As shown in Figure 4, the water could move downwards smoothly in the sandy soil column with greater porosity. The variation of the water content can be divided into initial, variation, and steady stages. The maximum moisture content of the sand above the inter-layer (9# sensor) was close to the saturated water content of 26.72%. This is because the infiltrated water in the upper part of the loam inter-layer accumulated for a short time period. The wetting front arrival times of 10# were prolonged about 250 minutes compared to 5#. The high clay particle loam inter-layer obviously slowed down the infiltration process.

The background values of the Br^- in the sand and silty loam were near 0 mg/kg. The maximum concentration of Br^- in the sandy soil was approximately 11 mg/kg (Figure 5(a)) and that of the silty loam was 25 mg/kg (Figure 5(b)). The '500 min line' in the 2# soil column showed that the concentration of Br^- increased with

depth. This is because the different soil textures had different permeability to water and solute. The changes in the soil structure mainly changed the flow-pore system, hindering the Br^- downward migration and further collection.

In the unsaturated zone, VOCs were a non-conserving component, and the diffusion process was exchanged between the water phase and solid phase (Lin & Hildemann 1995). At the initial infiltration stage, the soil moisture was low, and benzene mainly moved with the gas phase. The amount of benzene in the upper soil gradually increased and stabilized with water flux. The maximum concentration was 10 mg/kg in the 1# column (Figure 5(c)).

When the water flow approached the loam inter-layer, the velocity slowed down, and hindered the benzene migration, mainly in the form of liquid adsorption. The decrease in pore water velocity was accompanied by a decrease in the kinetic adsorption rate at the interface of the sand and silty clay materials (Sana & Jalila 2016). The concentration of benzene increased gradually, and reached the maximum value of 15 mg/kg at 40 cm in 500 min (Figure 5(d)). The retention ability of benzene in silty loam was greater than that of sand. It showed that the soil's adsorption and purification capacity for pollutants was negatively related to its grain size.

Breakthrough curves and discussion

The effective diffusion coefficient of the pollutants in the soil gas phase was less than that of the air because of the barrier function of the solid surface of the porous media and the skeleton (Huang 2002; Sana & Jalila 2016). The coefficient has a direct effect on the repair process of VOCs. The mass transfer from the unsaturated zone to the groundwater can be analysed by using an artificially instrumented facility (Jellali *et al.* 2001). BTC (breakthrough curves) refer to filling
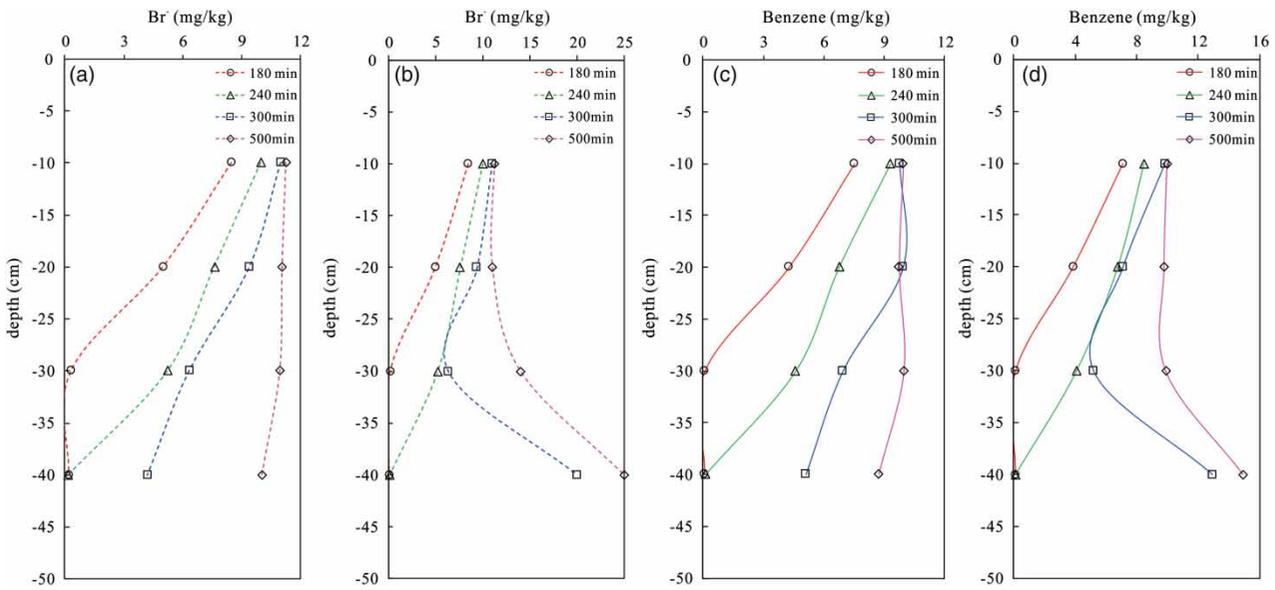
Figure 5 | Br⁻ concentration at different depths of two columns 1# (a) and 2# (b); benzene concentration at different depths of two columns 1# (c) and 2# (d).

the soil with a certain weight into the soil column and continuously injecting the solute. Then, the curve between the relative concentration of the solute and time is obtained (Wambold 1993; Zheng & Gordon 1998). The BTC can be used to solve the migration parameters, such as the hydrodynamic dispersion coefficient and the pore flow velocity. The BTC of the various petroleum compounds can be measured using different materials in soil column experiments, and the retardation factors for organic compounds can be determined (Larsen *et al.* 1992). It can not only directly reflect the process of solute changes, but also reflect the interaction with the soil.

The Br⁻ BTC of the two soil columns are shown in Figure 6(a). The Br⁻ began to penetrate at T_0, which

indicated that the pollutant entered the aquifer through the unsaturated zone. The concentration of Br⁻ gradually stabilized over a relatively constant time $Ts(C/C_0 = 1)$, which indicated that the non-organic components in the sewage reach the aquifer through the unsaturated zone. The breakthrough of the Br⁻ in soil was greatly hindered by the addition of layered loam to the sandy soil. To achieve full breakthrough, the tracers needed to completely remove the deionized water from the non-moving water area through diffusion. The increased small pores increased the immovable area and the breakthrough time. The increased clay content led to the decrease of soil porosity and the increase of tortuosity. This decreased the speed of the water movement and increased the migration time of the
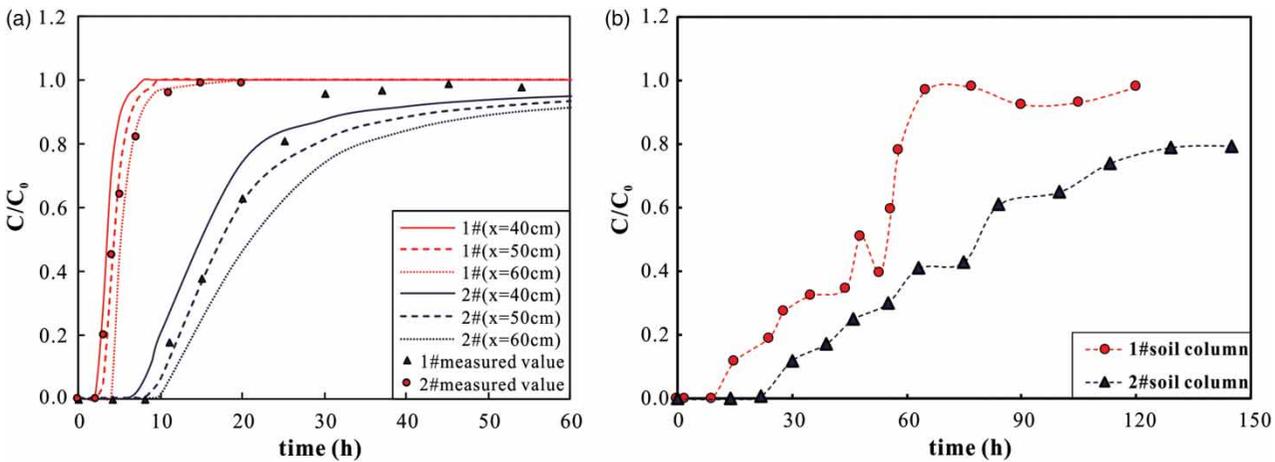

Figure 6 | (a) Fitting curves of the relative concentration of Br⁻ (the measured value of column: x = 50 cm); (b) benzene BTC of the two soil columns.

Table 6 │ Soil solute transport parameters

Column	$t_{0.16}$/h	$t_{0.5}$/h	$t_{0.84}$/h	$_{max}C/C_0$	ν/(cm·h^{-1})	D/(cm^2·h^{-1})
1$^{\#}$	2.8	4.33	7.25	0.99	11.547344112	1.499499591
2$^{\#}$	10.77	17.4	26.3	0.98	2.873563218	0.676999679

tracers, thus changing the shape of the BTC. Using the BTC to calculate the hydrodynamic dispersion coefficient was simple and straightforward using Equation (14). The results of the calculation are shown in Table 6.

According to erfc(x) Equation (12), the fitting curves between the C/C_0 of Br$^-$ and t were obtained and compared to the actual curves Figure 6(a).

The actual BTC curves were basically consistent with the general trend of the theoretical curves, which proved the validity and reliability of the soil column experiment.

The benzene BTC of the two soil columns are shown in Figure 6(b). The mobility of benzene in sand was greater than that in silty loam, and the equilibrium concentration of the 1# column was greater than that of the 2# soil column. This showed the obvious inter-layer adsorption and degradation of benzene. The retardation factors were calculated by Equation (14). The retardation factor of benzene was higher in the 1# soil column than in the 2# soil column (Table 7).

Because of the different solute characteristics of Br$^-$ and benzene, the BTC were different. Benzene as an adsorbent requires an adsorption process. Therefore, it showed accumulation in the loam inter-layer and reached maximum concentration until the adsorption equilibrium, at which point it reached complete penetration. The homogeneous sand layer in the unsaturated zone was more harmful to the groundwater. The increased clay particles in the soil inter-layer reduced the hydraulic conductivity and the speed of downward movement of the pollutants. Additionally, the parameters could be calculated through the soil column experiments, which can be used to quantitatively analyse the migration law of pollutants in the unsaturated zone.

Table 7 │ Retardation factor in the unsaturated zone column experiment

Column	$_{max}C/C_0$	t_c^*/h	t_c/h	R
1$^{\#}$	0.1	72	10	7.2
2$^{\#}$	0.08	120	32	3.75

CONCLUSIONS

In this paper, we discussed the effect of the loam inter-layer on benzene penetrating the vadose zone based on the basic adsorption experiments and the indoor seepage simulation soil column experiments, which can be summarized as follows:

(1) The adsorption of Br$^-$ to the soils was negligible ($1/n_{sand} = 21.32$; $1/n_{loam} = 9.66$). The adsorption equilibrium time of sand for benzene was higher than that of silty loam soil, and the adsorption capacity was higher. The adsorption isotherms were linear, with the Henry model fitting best. The partition coefficient $K_{loam} = 0.0523$ was higher than $K_{sand} = 0.0176$. The higher the clay particle content was, the lower the mobility of the pollutants. The effect of the anionic Br$^-$ on the adsorption of benzene was negligible.
(2) The inter-layer with high clay content weakened the downward migration. The migration of Br$^-$ was in accordance with the water flow, while the migration of benzene was not only influenced by water but also related to its properties as well as the soil texture. The maximum concentration was 10 mg/kg in the 1# column and 15 mg/kg in the 2# column at 40 cm in 500 min.
(3) The breakthrough test showed that the inter-layer had multiple effects on the polluted water. It not only delayed the migration time by about 48 h into the aquifer but also had an adsorption and degradation effect on benzene.

This experiment was assumed under sealed conditions such that the diffusion and transport mechanism of gaseous benzene in the open air was not considered. Secondly, the soil column experiment could only simulate the vertical one-dimensional transport of pollutants, and could not research the horizontal migration law of pollutants. Moreover, this experiment represented pollutant transport characteristics of identical or similar soil well. Soil pollution remediation projects should focus on the specific soil textures of the research areas and combine this consideration with hydrogeological conditions and laboratory experiments.

This will allow us to calculate the level and time of arrival of the pollutants by using the solute transport equation. Hence, this will facilitate the control of pollutants in groundwater and allow their later restoration.

ACKNOWLEDGEMENTS

REFERENCES

Abbas, T. R., Yu, J. H., Fen, C. S., Yeh, H. D. & Yeh, L. M. 2012 Modeling volatilization of residual VOCs in unsaturated zones: a moving boundary problem. *Journal of Hazardous Materials* **219–220** (12), 231–239.

Appelo, C. A. J. 1994 Mass balances and ecosystem dynamics. In: *Geochemistry Groundwater and Pollution*, 2nd edn. A A Balkema, Rotterdam, The Netherlands, pp. 46–58.

Aral, M. M. 1995 Influence of non-equilibrium sorption on contaminant transport. In: *Advances in Groundwater Pollution Control and Remediation*. Georgia Institute of Technology, School of Civil and Environmental Engineering. Kluwer Academic Publishers, Boston, Vol. 9, p. 23.

Ayotamuno, M. J., Kogbara, R. B., Ogaji, S. O. T. & Probert, S. D. 2006 Petroleum contaminated ground-water: Remediation using activated carbon. *Applied Energy* **83** (11), 1258–1264.

Bartelt-Hunt, S. L., Smith, J. A., Burns, S. E. & Rabideau, A. J. 2005 Evaluation of granular carbon, shale, and two organoclays for use sorptive amendments in clay landfill liners. *Journal of Geotechnical and Geoenvironmental Engineering* **131** (7), 848–856.

Blowes, D. W., Ptacek, C. J. & Jambor, J. L. 1997 In-situ remediation of chromate contaminated groundwater using permeable reactive walls: laboratory studies. *Environmental Science and Technology* **31** (12), 3348–3357.

Cooper, C., Jiang, J. & Ouki, S. 2010 Preliminary evaluation of polymeric Fe- and Al-modified clay as adsorbent for heavy metal removal in water treatment. *Journal of Chemical Technology and Biotechnology.* **77** (5), 546–551.

Duong, D. D. 1992 *Adsorption Analysis: Equilibria and Kinetics*. Department of Chemical Engineering, University of Queensland, Queensland, Australia, vol. 2, pp. 18–34.

Fetter, C. W. 2011 Chapter7- Organic compounds in groundwater. In: Contaminant *Hydrogeology*, 2nd edn (N. Q. Zhou & Y. Huang, eds). Higher Education Press, Beijing, pp. 278–282.

Flathman, P. E., Jerger, D. E. & Exner, J. H. 1994 *Bioremediation: Field Experience*. Lewis Publishers, New York, pp. 1–8.

Franco, M. A. E., Carvalho, C. B., Bonetto, M. M., Soares, R. P. & Liliana, A. F. 2017 Removal of amoxicillin from water by adsorption onto activated carbon in batch process and fixed bed column: kinetics, isotherms, experimental design and breakthrough curves modelling. *Journal of Cleaner Production* **161**, 947–956.

Gianfilippo, M. D., Costa, G., Verginelli, I., Gavasci, R. & Lombardi, F. 2016 Analysis and interpretation of the leaching behaviour of waste thermal treatment bottom ash by batch and column tests. *Waste Management* **56**, 216–228.

Gullick, R. W. & Weber, J. W. J. 2001 Evaluation of shale and organoclays as sorbent additives for low-permeability soil containment barriers. *Environment Technology* **35** (1), 1523–1530.

Huang, G. Q. 2002 *Transport of Organic Contaminants During Soil Vapor Extraction and Mathematic Simulations*. PhD thesis, School of Chemical Engineering, Tianjin University, Tianjin, China.

Jellali, S., Muntzer, P., Razakarisoa, O. & Schafer, G. 2001 Large scale experiment on transport of trichloroethylene in a controlled aquifer. *Transport in Porous Media* **44** (1), 145–163.

Kampe, M., Holfelder, T. & Montenegro, H. 2003 Identification and parameterization of flow processes in artificial capillary barriers. *Water Resource Research* **39** (10), 85–94.

Khan, A. M., Wick, L. Y., Harms, H. & Thullner, M. 2016 Biodegradation of vapor-phase toluene in unsaturated porous media: column experiments. *Environmental Pollution* **211**, 325–331.

Krishna, B. S., Murty, D. S. R. & Prakash, B. S. J. 2001 Surfactant-modified clay as adsorbent for chromate. *Applied Clay Science* **20** (1–2), 65–71.

Larsen, T., Kjeldsen, P. & Christensen, T. H. 1992 Sorption of hydrophobic hydrocarbons on three aquifer materials in a flow through system. *Chemosphere* **24** (4), 439–451.

Lin, J. S. & Hildemann, L. M. 1995 A nonsteady-state analytical model to predict gaseous emissions of volatile organic compounds from landfills. *Journal of Hazardous Materials* **40** (3), 271–295.

Lo, M. C. I., Mak, R. K. M. & Lee, S. C. H. 1997 Modified clays for waste containment and pollutant attenuation. *Journal of Environmental Engineering* **123** (1), 25–32.

Ma, L., Liu, Y. F., Zhang, J., Yang, Q., Li, G. H. & Zhang, D. Y. 2018 Impacts of irrigation water sources and geochemical conditions on vertical distribution of pharmaceutical and personal care products (PPCPs) in the vadose zone soils. *Science of the Total Environment* **626**, 1148–1156.

Mahmoodlu, M. G., Hassanizadeh, S. M., Hartog, N. & Raoof, A. 2014 Oxidation of trichloroethylene, toluene, and ethanol vapors by a partially saturated permeable reactive barrier. *Journal of Contaminant Hydrology* **164** (4), 193–208.

Nanta, P., Kasemwong, K. & Skolpap, W. 2018 Isotherm and kinetic modeling on superparamagnetic nanoparticles adsorption of polysaccharide. *Journal of Environmental Chemical Engineering* **6**, 794–802.

Onsy, A. M., And, M. & Paleologos, E. K. 2017 *Fundamentals of Geoenvironmental Engineering*. Butterworth-Heinemann

Technology & Engineering, Oxford, UK. Chapter 16 – Dielectric Permittivity and Moisture Content, pp. 581–637.

Parker, J. C. & Van Genuchten, M. T. 1984 *Determining Transport Parameters From Laboratory and Field Tracer Experiments*. Federal University of Rio de Janeiro, Rio de Janeiro, Brazil. Blacksburg ResearchGate, 27 pp.

Petersen, L. W., Rolston, D. E., Moldrup, P. & Yamaguchi, T. 1994 Volatile organic vapor diffusion and adsorption in soils. *Journal Environmental Quality* **23** (4), 799–805.

Porro, I., Wierenga, P. J. & Hills, R. G. 1993 Solute transport through large uniform and layered soil columns. *Water Resources Research* **29** (4), 1321–1330.

Rivett, M. O., Wealthall, G. P., Dearden, R. A. & McAlary, T. A. 2011 Review of unsaturated-zone transport and attenuation of volatile organic compound (VOC) plumes leached from shallow source zones. *Journal of Contaminant Hydrology* **123** (3), 130–156.

Ronen, D., Graber, E. R. & Laor, Y. 2005 Volatile organic compounds in the saturated unsaturated interface region of a contaminated phreatic aquifer. *Vadose Zone Journal* **4** (2), 337–344.

Sana, D. & Jalila, S. 2016 Combined effect of unsaturated soil condition and soil heterogeneity on methylene blue adsorption/desorption and transport in fixed bed column: experimental and modeling analysis. *Journal of King Saud University-Science* **28** (4), 308–317.

Sander, R. 2015 Compilation of Henry's law constants (version 4.0) for water as solvent. *Atmospheric Chemistry Physics* **15** (8), 4399–4981.

Sheng, G. Y., Xu, S. H. & Boya, S. A. 1996 Mechanism(s) controlling sorption of neutral organic contaminants by surfactant-derived and neutral organic matter. *Environmental Science and Technology* **30** (5), 1553–1557.

Song, X. M., Wen, Y. J., Wang, Y. Y., Adeel, M. & Yang, Y. S. 2018 Environmental risk assessment of the emerging EDCs contaminants from rural soil and aqueous sources: analytical and modelling approaches. *Chemosphere* **198**, 546–555.

Suthersan, S. S. 2002 *Chapter1-Hazardous Wastes Pollution and Evolution of Remediation in Natural and Enhanced Remediation Systems*. Lewis Publishers, New York, pp. 1–11.

Unger, D. R., Lam, T. T., Schaefer, C. E. & Kosson, D. S. 1996 Predicting the effect of moisture on vapour-phase sorption of volatile organic compounds to soils. *Environment Science & Technology* **30** (4), 1081–1091.

Van Genuchten, M. T. 1980 A close-form equation for predicting the hydraulic conductivity of unsaturated soil. *Soil Science Society of America Journal* **44**, 892–898.

Walter, M. T., Kim, J. S., Steenhuis, T. S., Parlange, J. Y., Heilig, A., Braddock, R. D., Selker, J. S. & Boll, J. 2000 Funneled flow mechanisms in a sloping layered soil: laboratory investigations. *Water Resources Research* **36** (4), 841–849.

Wambold, W. S. 1993 *Large and Small Scale Laboratory Tests: for VOC Transport Through Compacted Clay*. MS thesis, University of Wisconsin at Madison, pp. 103–106.

Yang, M. D. & Yanful, E. K. 2002 Water balance during evaporation and drainage in cover soils under different water table conditions. *Advances in Environmental Research* **6** (4), 505–521.

Zhang, Z. F., Strickland, C. E. & Link, S. O. 2017 Design and performance evaluation of a 1000-year evapotranspiration-capillary surface barrier. *Journal of Environmental Management* **187**, 31–42.

Zheng, C. M. & Gordon, D. B. 1998 In: *Applied Contaminant Transport Modeling* (G. P. Lu & J. Y. Sun, eds). Department of Geological Sciences, University of Alabama, USA, pp. 24–49.